

Processing and Properties of TiB₂ with MoSi₂ Sinter-additive: A First Report

T. S. R. Ch. Murthy, B. Basu,[†] and R. Balasubramaniam

Department of Materials and Metallurgical Engineering, Indian Institute of Technology, IIT-Kanpur, India

A. K. Suri, C. Subramanian, and R. K. Fotedar

Material Processing Division, Bhabha Atomic Research Center, Mumbai, India

The densification of non-oxide ceramics like titanium boride (TiB₂) has always been a major challenge. The use of metallic binders to obtain a high density in liquid phase-sintered borides is investigated and reported. However, a non-metallic sintering additive needs to be used to obtain dense borides for high-temperature applications. This contribution, for the first time, reports the sintering, microstructure, and properties of TiB₂ materials densified using a MoSi₂ sinter-additive. The densification experiments were carried out using a hot-pressing and pressureless sintering route. The binderless densification of monolithic TiB₂ to 98% theoretical density with 2–5 μm grain size was achieved by hot pressing at 1800°C for 1 h in vacuum. The addition of 10–20 wt% MoSi₂ enables us to achieve 97%–99% ρ_{th} in the composites at 1700°C under similar hot-pressing conditions. The densification mechanism is dominated by liquid-phase sintering in the presence of TiSi₂. In the pressureless sintering route, a maximum of 90% ρ_{th} is achieved after sintering at 1900°C for 2 h in an (Ar+H₂) atmosphere. The hot-pressed TiB₂-10 wt% MoSi₂ composites exhibit high Vickers hardness (~26–27 GPa) and modest indentation toughness (~4–5 MPa·m^{1/2}).

I. Introduction

TITANIUM BORIDE (TiB₂) is a potential candidate material for high-temperature structural applications because of an excellent combination of properties such as high melting point (~3200°C), high thermal conductivity (60–120 W·(m·K)⁻¹), high elastic modulus (~500 GPa), and high hardness (25–32 GPa).¹ Despite having the above-cited useful combination of properties, the applications of monolithic TiB₂ are rather limited because of poor sinterability and exaggerated grain growth at high temperature. To overcome this problem, various metallic and non-metallic binders are used to obtain dense borides.

Extensive research has been reported in the open literature on the role of metallic binders in the densification of TiB₂. Ferber *et al.*² have used up to 10 wt% Ni to achieve more than 99% theoretical density by the hot-pressing route (1425°C). The strength and toughness of TiB₂ ceramics are significantly enhanced with a finer grain size (4 μm) and low Ni content (<2 wt%).² Kang *et al.*³ observed that simultaneous addition of 0.5 wt% Fe and 0.5 wt% Cr enhances the densification of TiB₂ in the temperature range of 1800°–1900°C. They have shown that when a small amount of Fe (0.5 wt%) is added, abnormal grain growth occurs and the sintered density is low. In the case

of addition of B₄C along with 0.5 wt% Fe, abnormal grain growth was suppressed considerably, and an increase in sintered density up to 95% ρ_{th} was measured.⁴ However, the presence of a metallic binder is not desirable for high-temperature structural applications. Therefore, non-metallic sinter-additives need to be used, with an aim to improve sinterability and also to retain high-temperature properties with good oxidation resistance.

Different non-metallic additives such as AlN,⁵ ZrO₂,^{6–12} SiC,^{8,10,12,13} Si₃N₄,¹⁴ CrB₂,¹⁵ B₄C,^{9,16} TaC,¹⁷ TiC,^{17,18} WC,¹⁷ TiN,¹⁷ ZrN,¹⁷ and ZrB₂¹⁷ have been used for attaining densification of TiB₂ with good mechanical properties. Torizuka and Kishi⁸ and Torizuka *et al.*¹² observed the formation of grain-boundary liquid phase (amorphous SiO₂) when SiC was used as an additive. Moreover, they identified the presence of a partial liquid phase, (Ti,Zr)₅Si₃, at triple points in a TiB₂-19.5 wt% ZrO₂-2.5/5.0 wt% SiC composite processed via the hot isostatic pressing (HIP) route. Watanabe and Shoubu¹⁹ reported the formation of a (Ti,Zr)B₂ solid solution in hot-pressed TiB₂-30 wt% ZrO₂ composites. Telle *et al.*⁶ also observed the formation of a (Zr,Ti)O₂ solid solution in addition to a (Ti,Zr)B₂ solid solution, when 25 vol% ZrO₂ was added to TiB₂. In another interesting investigation, Torizuka *et al.*¹⁰ did not report any solid solution formation when 20 wt% ZrO₂ binder was used to densify TiB₂ via the HIP route. According to Murata *et al.*,¹⁷ TaC and TaN were quite effective in densifying TiB₂. In their work, (Ti,Ta)B₂ and (Ta,Ti)(C,N) solid solutions were observed to form after hot pressing at 2000°C, when TaC was added to TiB₂. Li *et al.*⁵ identified the formation of BN, TiN, and Al₂O₃ phases in a TiB₂-20 wt% AlN composite, fabricated by hot pressing at 1800°C. In another work, Ho Park *et al.*¹⁴ reported the formation of different reaction products like TiN and BN in TiB₂-2.5–10 wt% Si₃N₄ composites (sintered at 1800°C), and observed that Si₃N₄ acts as a grain growth inhibitor.

Among various high-temperature intermetallics, MoSi₂ has a high thermal conductivity (~53 W·(m·K)⁻¹) and good oxidation resistance (up to 1400°C).²⁰ Additionally, MoSi₂ is reported to have good thermo-mechanical compatibility with TiB₂,²⁰ as can also be predicted from the small mismatch in the thermal expansion co-efficient (8.1 × 10⁻⁶ K⁻¹ for TiB₂¹ and 8.5 × 10⁻⁶ K⁻¹ for MoSi₂).²⁰ While MoSi₂ can be a potential reinforcement/sinter-additive for developing TiB₂ materials for high-temperature applications, no attempt, according to the best of the authors' knowledge, has been made to assess such a feasibility. In this perspective, the present work reports the processing, microstructure, and mechanical properties of TiB₂-MoSi₂ composites.

II. Experimental Procedure

(1) Processing

TiB₂ and MoSi₂ powders, prepared in the laboratory, were selected as starting powders for composite production. The mean particle diameter and particle size distribution of both the TiB₂

R. Koc—contributing editor

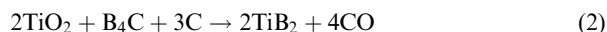
Manuscript No. 20324. Received October 31, 2004; approved June 8, 2005. Supported by Board of Research in Nuclear Science (BRNS) programme of Department of Atomic Energy (DAE), Government of India.

[†]Author to whom correspondence to addressed. e-mail: bikram@iitk.ac.in

and MoSi₂ powders were measured using a laser particle size analyzer (Analsette 22, Fritsch, Germany). The specific surface area was obtained using the BET (Coulter, Miami, FL, SA300) method. In the production of TiB₂ powders, B₄C powders, synthesized in our laboratory are used. B₄C powders were processed using carbothermic reduction of commercial boric acid (H₃BO₃, laboratory reagent grade):



Carbon, used in the above reaction, was commercially available high-purity (>99% purity) petroleum coke (M/S Assam carbon, Guwahati, India). The size of the coke was –325 mesh size, and loss on ignition (LOI) of the coke used was found to be < 0.5%. During the initial stage of reaction (1), H₃BO₃ is reduced to form B₂O₃, which, above 1200°C, is further reduced by carbon to form B₄C lumps. These lumps are mechanically crushed and ball milled to produce fine powders, which are purified by acid leaching followed by washing with water to remove impurities. The details of B₄C powder production can be found elsewhere.²¹ As part of the present work, TiB₂ powder was produced by a borothermic reaction, as follows:



Oxygen and carbon, the major impurities in as-synthesized TiB₂, were determined by the vacuum fusion analysis technique (Leco Industries). The details of the starting powders are summarized in Table I.

The synthesized TiB₂ powder was further ground to break down the agglomerates to form finer particles having a *D*₅₀ around 1.1 μm. MoSi₂ was synthesized from elemental powders of Mo (>99% purity, Leco Industries) and Si (>99% purity, Merck, Germany). Mechanical grinding further reduced the size of the synthesized MoSi₂ powders, leading to a finer particle size with a *D*₅₀ around 1.4 μm. SEM images of the starting powders are shown in Fig. 1. While finer equiaxed TiB₂ particles can be observed in Fig. 1(a), some agglomerated MoSi₂ particles can be noted in Fig. 1(b). To this end, it can be noted that an alternative route to obtain submicrometer TiB₂ is reported elsewhere.²²

Approximate amounts of boride and silicide powders of various compositions (0, 10, 15, 20, and 25 wt% MoSi₂) were mixed using WC grinder. The densification was performed by hot pressing for 1 h in vacuum (10⁻⁵ Pa), using a 10 mm diameter graphite die at 32 MPa pressure. The samples were hot pressed at 1700°C at a heating rate of 15°C/min. Selected experiments were also carried out at 1650° and 1800°C. After completion of sintering, vacuum and pressure were maintained till the end of cooling. The thickness of the hot-pressed pellets was around 6–8 mm.

To study the feasibility of densification via the pressureless sintering route, the green pellets of various TiB₂–MoSi₂ composites (without organic binder) were used. The green density of the cold-pressed specimens was 65% of the theoretical density. The green samples were sintered for 2 h at 1900°C at a heating rate of 15°C/min in a reducing atmosphere (Ar+H₂). Prior to the sintering experiments, the vacuum chamber was evacuated and backfilled with Ar to ensure that no residual oxygen was present.

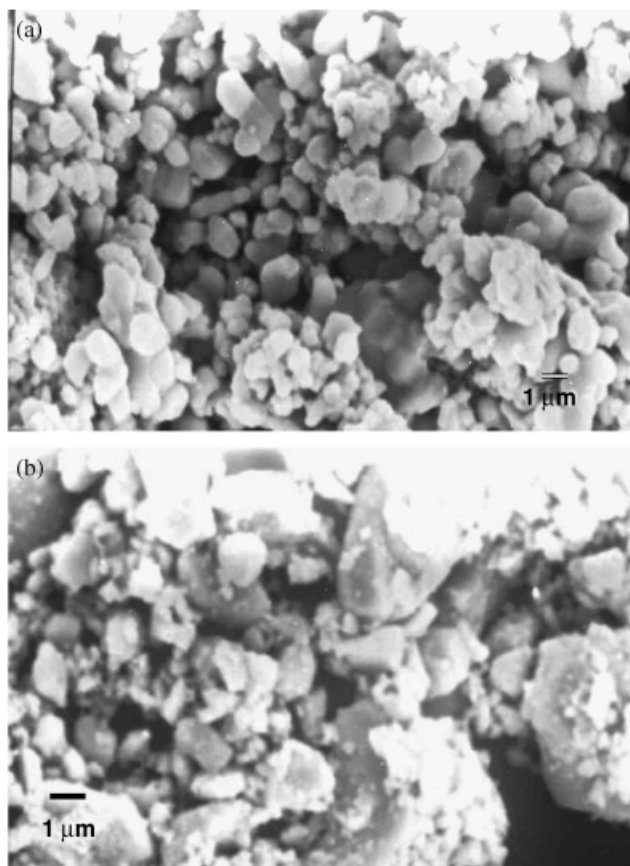


Fig. 1. SEM images showing the morphology of starting powders: (a) titanium boride (TiB₂) and (b) MoSi₂.

(2) Microstructure and Mechanical Properties Characterization

The cleaned dense pellets were weighed, and the density was measured in water using the Archimedes principle. The crystalline phases in the starting powders and hot-pressed sample were analyzed using XRD (Rich-Seifert, Germany, 2000D). Microstructural investigation of the phase assemblage was performed by means of SEM on polished and fractured surfaces. Detailed microstructural analysis was carried out using EPMA (WDS analysis) and 200 kV TEM (JEM 2000 FX, JEOL, Tokyo, Japan). A thin foil for TEM was prepared following standard ion beam thinning procedures.

The mechanical properties were measured only for hot-pressed samples. The Vickers hardness on the smoothly polished hot-pressed samples was obtained with a load of 10 kg (dwell time 15 s). The indentation fracture toughness (*K*_{IC}) data were evaluated by crack length measurement of the crack pattern formed around Vickers indents, adopting the model formulation proposed by Anstis *et al.*²³: $K_{IC} = 0.016(E/H)^{1/2}P/c^{3/2}$, where *E* is the Young's modulus, *H* the Vickers's hardness, *P* the applied indentation load, and *c* the half crack length. The reported values are the average of five indentation tests.

Table I. Details of the Starting Powders Used in the Present Work

Powder	Supplier	Carbon (wt%)	Oxygen (wt%)	Nitrogen (wt%)	Metallic Impurities (wt%)	Median particle diameter, <i>D</i> ₅₀ (μm)	Surface area (m ² /g)
TiB ₂	In-house	0.6	0.5	0.6	—	1.1	1.360
MoSi ₂	In-house	0.37	0.3	—	—	1.4	0.389
TiO ₂	Merck (Germany)	—	—	—	Pb ≤ 0.005 As ≤ 0.0005 Fe ≤ 0.005	0.8	—
B ₄ C	In-house	19.5	<1.0	—	Fe ~ 2000 ppm Si ~ 2000 ppm	6.7	—

TiB₂, titanium boride.

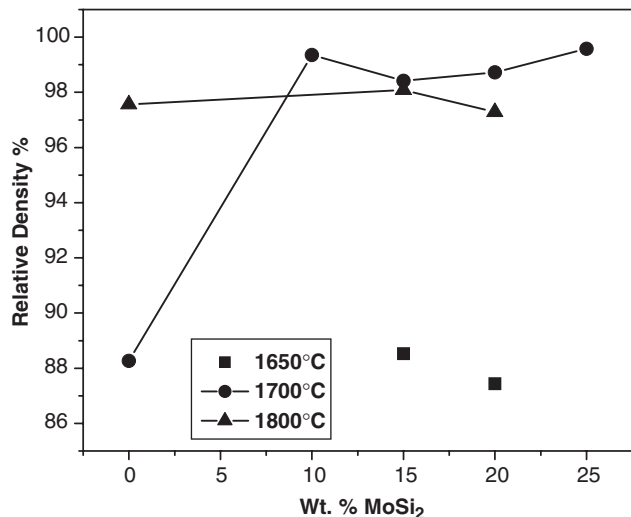


Fig. 2. Relative density of hot-pressed samples as a function of MoSi₂ content. The lines joining the data points are connecting the densification data obtained at varying hot-pressing temperatures.

It should be mentioned here that the measured toughness is dependent on the test technique, which are widely classified into long- and short-crack methods. Short-crack techniques involve measurement of the crack lengths (radial/median) around hardness indentations, from which the toughness is computed using established formulas.^{23,24} Although the loading conditions are less well characterized and crack growth is “slow” relative to conventional long crack fracture toughness tests, careful use can yield reproducible results for indentation toughness measurements.

In view of the above as well as to validate the indentation toughness data, another established model proposed by Palmqvist²⁴ was also used: $K_{Ic} = 0.0089(E/H)^{2/5}P/(al^{1/2})$, where a is the half diagonal length, and $l = c - a$. It can be noted that Palmqvist's formula is valid for $0.25 < l/a < 2.5$.

III. Results

(1) Densification

(A) *Hot Pressing*: The densification data of the hot-pressed samples are presented in Fig. 2. For monolithic TiB₂, a poor densification of ~88% theoretical density (ρ_{th}) was obtained after hot pressing at 1700°C, while an excellent densification of ~98% ρ_{th} was achieved at 1800°C. The density and the material property data (literature data and present work) of monolithic TiB₂ as well as TiB₂ sintered with various sinter-additives are summarized in Table II. Observing the data in Table II, it is apparent that there have been few attempts to densify TiB₂ without any sinter-additive. Earlier, a maximum of 90%

Table III. Details of the Densification Data for Ceramic Samples, Pressureless Sintered at 1900°C for 2 h in an (Ar+H₂) Atmosphere

Sample designation*	Theoretical density (g/mL)	Density (g/mL)	Relative density (%)	% weight loss
PS10	4.65	3.83	82.36	4.4
PS15	4.71	4.00	84.92	5.0
PS20	4.78	4.23	88.49	5.6
PS25	4.85	4.43	91.34	6.2
PS0	4.52	Not densified	Not densified	Not densified

*PS, pressureless sintered sample. Digit represents composition: 10—10% MoSi₂+TiB₂; 15—15% MoSi₂+TiB₂; 20—20% MoSi₂+TiB₂; 25—25% MoSi₂+TiB₂; 0—0% MoSi₂+TiB₂. TiB₂, titanium boride.

ρ_{th} was reported to be obtained for monolithic TiB₂ after hot pressing at 1800°C for 1 h in Argon.¹⁴ The attainment of ~98% ρ_{th} at 1800°C, in the present case, for binderless TiB₂ by the hot-pressing route is a new result.

Critical observation of the data presented in Fig. 2 reveals that the sintered density of TiB₂ increases with the amount of MoSi₂ sinter-additive, and a maximum of 99% ρ_{th} can be obtained with 10% MoSi₂ addition after hot pressing at 1700°C. For 20% MoSi₂-reinforced composites, a similar high density of around 98% ρ_{th} is obtained at 1700°C. Additional hot-pressing experiments at 1700°C revealed that 98%–99% ρ_{th} can be obtained with 15% and 25% MoSi₂ additions. From the above observations, it should be clear that MoSi₂ improves the sinterability of TiB₂ and more than 95% ρ_{th} can be obtained by the hot-pressing route at a lower temperature of 1700°C. Considerable weight loss (during hot pressing) of around 4%–9% is measured depending on the sintering temperature and MoSi₂ content.

Because of the excellent densification achieved with a higher amount of MoSi₂ additions and in order to study the feasibility of densifying them at lower temperature, limited experiments were carried out by hot pressing TiB₂-15% MoSi₂ and TiB₂-20% MoSi₂ composites at lower temperature of 1650°C for 1 h. The densification results reveal that 87%–89% ρ_{th} can be obtained for these composites with a lower density for higher silicide additions.

(B) *Pressureless Sintering*: Table III presents the densification results of pressureless sintering experiments, carried out at 1900°C for 1 h in an inert (Ar+H₂) atmosphere. The sintered density of the composites increases with increasing MoSi₂ addition. A maximum sintered density of 91% ρ_{th} is obtained with 25 wt% MoSi₂ addition. The weight loss during sintering varies between 4.4 and 6.2 wt% for different MoSi₂ additions and the measured weight loss is observed to increase with an increase in MoSi₂ content. From the obtained results, it is evident that pressureless sintering cannot be adopted to densify TiB₂ even at

Table II. Density, Hardness, and Fracture Toughness of the Newly Developed TiB₂-Based Materials

Material	Processing details	Relative density (% ρ_{th})	Vickers hardness (H_v), GPa	Indentation toughness (K_{Ic}), MPa·m ^{1/2}	References
Monolithic TiB ₂	HP 1800°C, 1 h, Argon	90	23	5.8	Ho Park <i>et al.</i> ¹⁴
TiB ₂ -2.5% Si ₃ N ₄	HP 1800°C, 1 h, Argon	99	27	5.1	Ho Park <i>et al.</i> ¹⁴
TiB ₂ -10% Si ₃ N ₄	HP 1800°C, 1 h, Argon	96	20	4.4	Ho Park <i>et al.</i> ¹⁴
TiB ₂ -5% AlN	HP 1800°C, 1 h, Argon	98	22	6.8	Li <i>et al.</i> ⁵
TiB ₂ -10% AlN	HP 1800°C, 1 h, Argon	88.5	14	5.2	Li <i>et al.</i> ⁵
TiB ₂ -2.5% SiC	PS 1700°C, vacuum and HIP, 1600°C, Argon	96	—	4.3	Torizuka <i>et al.</i> ¹³
Monolithic TiB ₂	HP 1800°C, 1 h Vacuum	97.5	26	5.1	Present work
TiB ₂ -10% MoSi ₂	HP 1700°C, 1 h Vacuum	99.3	27	4.0	Present work
TiB ₂ -20% MoSi ₂	HP 1700°C, 1 h Vacuum	98.7	25	5.0	Present work

For comparison, the literature data are also mentioned. Different processing routes are also indicated. TiB₂, titanium boride; HP, hot pressing; PS, pressureless sintering; HIP, hot isostatic pressing.

a high temperature of 1900°C, and large addition of MoSi₂ does not aid in obtaining TiB₂-MoSi₂ with closed porosity i.e., with more than 95% ρ_{th} sintered density.

A summary of the experimental results clearly indicates that the densification of TiB₂ is enhanced with the addition of MoSi₂ content at a lower hot-pressing temperature of 1700°C. With pressureless sintering, a maximum of 91% ρ_{th} could be obtained at 1900°C for TiB₂-25% MoSi₂ composites.

As the major purpose of the material development work is to obtain dense borides with minimal sinter-additive content, detailed microstructural and mechanical properties were investigated for selected hot-pressed composites with 10% and 20% silicide additives. A comparison has also been made with the monolithic borides.

(2) Microstructure and Properties

XRD analyses of starting powders and hot-pressed specimens were carried out, and the results are shown in Fig. 3. These results indicate that the microstructure of the developed composites predominantly contain TiB₂ and MoSi₂. However, addition of 10 and 20 wt% MoSi₂ resulted in the formation of a small amount of TiSi₂. No presence of TiO₂ or SiO₂ or other Mo-silicide is observed within the detection limit of XRD.

The SEM image of fracture surfaces of monolithic TiB₂, hot pressed at 1800°C for 1 h, is shown in Fig. 4(a). The average

grain size of the monolithic TiB₂ particles in hot-pressed samples is around 2–5 μm (Fig. 4(a)). Considering the starting particle size of TiB₂ ($D_{50} \sim 1.1 \mu\text{m}$), this observation indicates that hot pressing at 1800°C does not promote any significant grain growth. The topography of the fracture surface (Fig. 4(a)) indicates that the transgranular fracture is the predominant mode of fracture. TEM investigation of the TiB₂-20% MoSi₂ composite was carried out, and representative bright field TEM images of the TiB₂-20% MoSi₂ composite is presented in Figs. 4(b)–(d). The presence of finer TiB₂ grains with sizes of 1–2 μm or less can be noticed along with the dispersion of coarser MoSi₂ particles (Figs. 4(b) and (c)). The typical aspect ratio of elongated silicides particles is around 4–5. Some equiaxed-shaped MoSi₂ particles, with sizes around 1 μm and having sharp interfaces with TiB₂ grain, can be observed in Fig. 4(c). The presence of a crystalline phase at the triple pocket is observed at grain-boundary triple pockets (Fig. 4(d)). EDS analysis (not shown) from the pocket phase reveals a strong Ti peak along with a weaker Si signal. The presence of Mo or B was not detected. The weaker Si signal may be because of the smaller size of the pocket phase and/or the use of a Si detector. More detailed TEM analysis of the investigated composite using high-resolution microscopy is presented elsewhere.²⁵ The above observation along with the XRD results suggests that TiSi₂, a reaction product, forms at grain-boundary triple pockets during sintering.

The mechanical properties, in particular hardness and fracture toughness, were measured for the selected hot-pressed materials using the Vickers indentation technique. A comparison of the mechanical properties of the newly developed materials with the TiB₂ sintered using various non-metallic additives is made in Table II. The Vickers hardness, recorded using 100 N indent load, is plotted against the MoSi₂ content in Fig. 5. The error bar in the hardness and toughness data indicates the standard deviation in the measurement with five indentations. While monolithic TiB₂ exhibits an average hardness of 26 GPa, a slightly lower hardness of 25 GPa is recorded for TiB₂-20% MoSi₂ composites. A high hardness of 26 GPa in monolithic binderless TiB₂ is a promising result, and this is attributed to the use of extremely finer TiB₂ particles. Also, the absence of hardness enhancement in the composites is because of the lower hardness of the MoSi₂ phase (≈ 10 GPa for pure MoSi₂) as well as the presence of another brittle intermetallic phase, TiSi₂. It can be noted here that high hardness of 19, 22–23, and 28 GPa were also reported for TiB₂-10 vol% B₄C,⁹ TiB₂-15 wt% TiC,¹⁷ and TiB₂-3 wt% CrB₂¹⁵ composites, respectively.

Based on the indentation crack length measurements and assuming theoretical *E*-modulus values for TiB₂ and TiB₂-MoSi₂ composites, the indentation toughness was evaluated. Table IV presents all the indentation data, as measured from SEM images of the indented surfaces. In order to study the reliability of the indentation toughness, the models proposed by Anstis *et al.*²³ as well as Palmqvist²⁴ were used. As the normalized crack length parameter, "*l/a*," lies between 0.25 and 2.5, the model proposed by Palmqvist was also used to compute indentation toughness in the present work. In fact, the crack length measurement reveals that the ratio (*l/a*) is usually more than 1.5. A critical look at Table IV indicates that the ranking of the investigated materials in terms of indentation toughness remains the same, independent of the model used to compute toughness. However, the toughness measured using Anstis *et al.*'s model underestimates the toughness and hence these values are considered while comparing the material properties with earlier developed TiB₂, sintered using various non-metallic additives (see Table II). The toughness of the investigated materials, measured using the model of Anstis *et al.*, varies in the range of 4–6 MPa·m^{1/2}. While the average toughness of monolithic TiB₂ and TiB₂-20% MoSi₂ lies around 5.1 MPa·m^{1/2}, a little lower toughness of 4.3 MPa·m^{1/2} was recorded for TiB₂-10% MoSi₂ composites. The toughness improvement in composites is not achieved primarily because of the presence of brittle ceramic phases like MoSi₂ and small amount of TiSi₂.

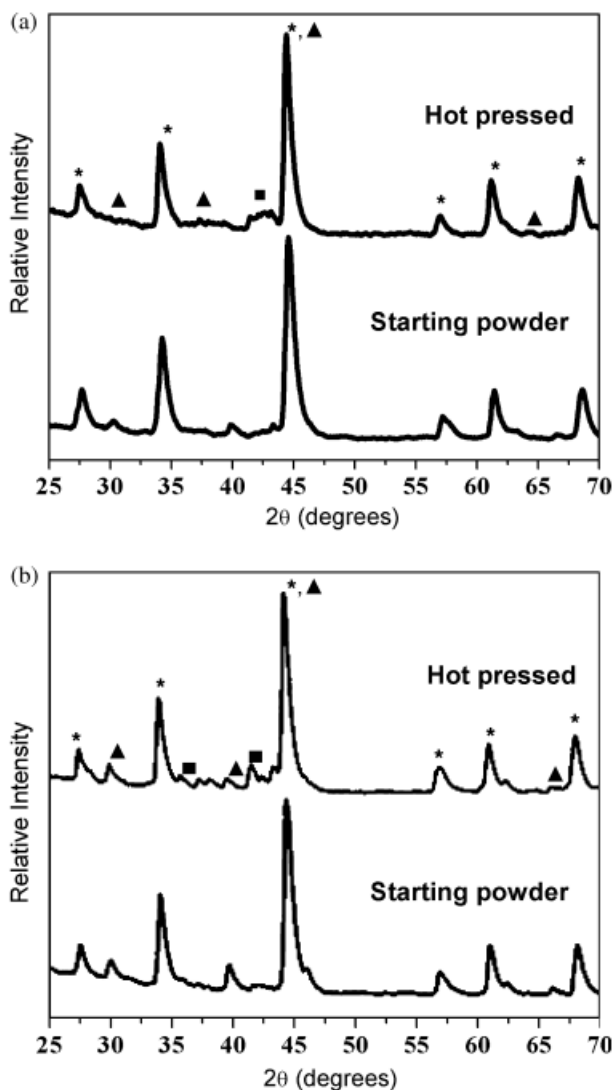


Fig. 3. Phase analysis of starting powder and hot-pressed samples (a) titanium boride (TiB₂)-10 wt% MoSi₂ and (b) TiB₂-20 wt% MoSi₂. The different crystalline phases are identified: TiB₂ (*); MoSi₂ (▲); TiSi₂ (■).

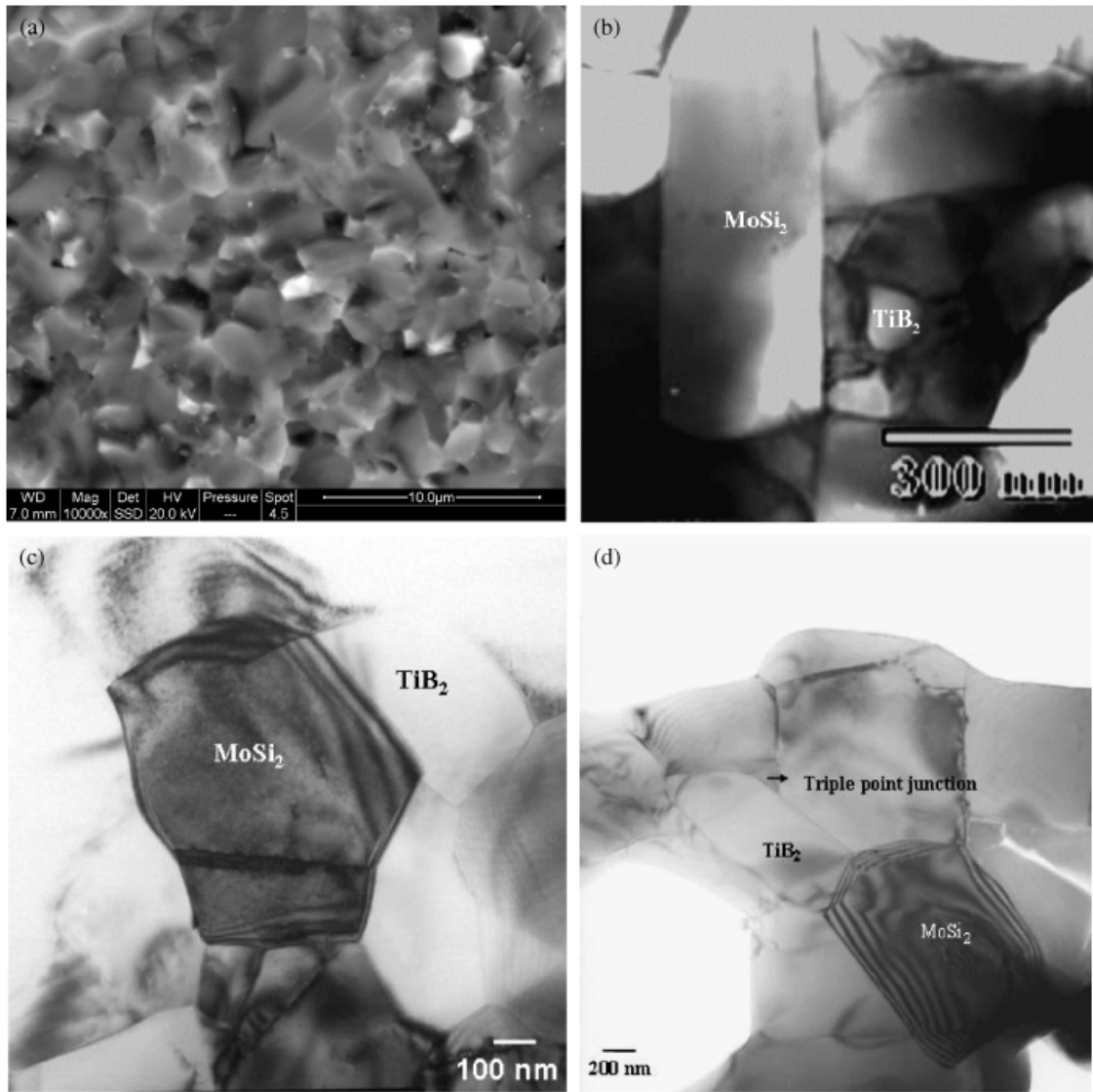


Fig. 4. SEM image of the fracture surface of monolithic titanium boride (TiB_2), hot pressed at 1800°C for 1 h (a). Bright field (BF) TEM image of TiB_2 -20 wt% MoSi_2 composite (b) and (c), hot pressed at 1700°C for 1 h. High-magnification BF TEM image revealing the presence of a crystalline phase at grain-boundary triple pocket (indicated by an arrow) (d).

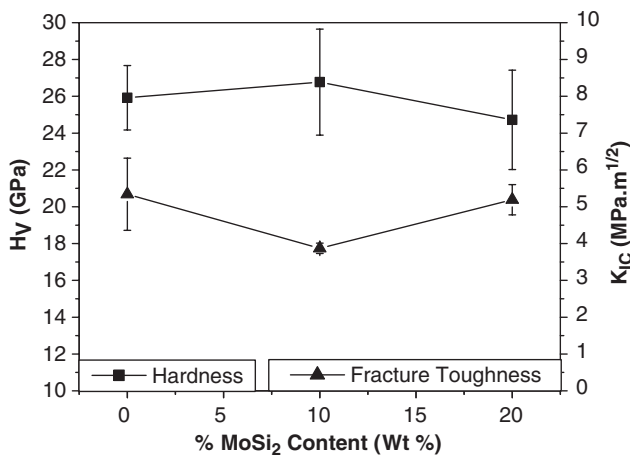


Fig. 5. Vickers hardness and indentation toughness as a function of MoSi_2 content. Monolithic titanium boride (TiB_2) is sintered at 1800°C , whereas the composites containing MoSi_2 are hot pressed at 1700°C .

IV. Discussion

In this section, an explanation for the high density obtained with monolithic TiB_2 as well as enhancement in densification of TiB_2 - MoSi_2 composites will be presented. Additionally, the mechanical properties, obtained with the newly developed materials, will be discussed with particular reference to the earlier work.

(1) Densification Mechanism

The better densification of monolithic TiB_2 can be explained on the basis of the particle size effect on sintering. As no binder/sinter-additive is used, the densification, in the present case, is governed by a solid-state sintering mechanism. The sintering kinetics strongly depends on the neck growth rate during the densification process. Following the classical two-particle sintering model,²⁶ the neck growth in case of solid-state sintering of monolithic TiB_2 can be explained following the classical relationships:

$$\left(\frac{x}{r}\right)^6 = \left[\frac{192\delta\gamma D_b\Omega}{KT}\right] \frac{t}{r^4} \tag{3}$$

$$\left(\frac{x}{r}\right)^5 = \left[\frac{80\gamma D_1\Omega}{KT}\right] \frac{t}{r^3} \tag{4}$$

Table IV. Summary of the Indentation Data i.e., Average Indent Diagonal Length and Total Crack Length as well as the Fracture Toughness Values, Computed using Models Proposed by Anstis et al.²³ and Palmqvist,²⁴ for the Investigated Materials

Material designation	Indent diagonal (2a), μm	Crack length (2c), m	l/a	Indentation toughness, $\text{MPa} \cdot \text{m}^{1/2}$ (Anstis et al.)	Indentation toughness, $\text{MPa} \cdot \text{m}^{1/2}$ (Palmqvist)
TiB ₂	84.4	245.2	1.9	5.1	7.5
TiB ₂ -10MoSi ₂	82.3	281.4	2.4	4.0	6.7
TiB ₂ -20MoSi ₂	86.1	231.8	1.7	5.0	7.1

Another crack length parameter (l) is defined as $l = c - a$. TiB₂, titanium boride.

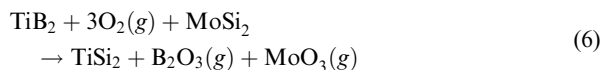
where D_l is the lattice self-diffusion coefficient for the rate-limiting diffusing species, D_b is the boundary self-diffusion coefficient for the rate-limiting diffusing species, δ is the boundary thickness, K is the Boltzman constant, Ω is the vacancy volume, x is the neck dimension, t is the time of sintering, T is the temperature during sintering, γ is the surface energy, and r is the particle size of the powders.

While Eq. (3) is derived for the intermediate stage of sintering in which the neck growth is controlled by grain-boundary diffusion, Eq. (4) is related to the lattice diffusion-controlled neck growth process occurring at the final stage of sintering.²⁶ From Eqs. (3) and (4), it is evident that the neck growth rate increases significantly with little reduction in particle size. Thus, one can intuitively expect a large increase in the densification rate, in the present case, with the use of finer TiB₂ particles (average size $\sim 1 \mu\text{m}$).

Comparing the data presented in Fig. 2 and Table II, it should be clear that MoSi₂, like other ceramic additives (Si₃N₄, AlN, SiC), can be effectively used as a sinter-additive to densify TiB₂-based materials. In fact, the use of MoSi₂ enables to achieve high densification even at a lower hot press temperature of 1700°C, when compared with earlier literature results (see Table II). To this end, it can be noted that 98% ρ_{th} was obtained with TiB₂-5 wt% AlN, hot pressed at 1800°C by Li et al.⁵ Ho Park et al.¹⁴ achieved 99% ρ_{th} using 2.5 wt% Si₃N₄ additives for TiB₂ hot pressed at 1800°C for 1 h. Thus, comparing our experimental results with literature reports, it can be said that high density obtained in TiB₂-10 wt% MoSi₂ composites at 1700°C, in the present case, is a new and promising result.

The existence of the grain triple pocket phase (TiSi₂) provides a useful insight into the densification mechanism. As the melting point of TiSi₂ is 1500°C, liquid TiSi₂ presumably forms during hot pressing (sintering temperature of 1700°C). It is reported in the literature that a surface layer of TiO₂ and B₂O₃ exists on the surface of TiB₂ particles, and B₂O₃ vaporizes rapidly above 1127°C.²⁷ In our hot-pressing experiments, 4%–6% weight losses are measured and this can be attributed to the evaporation of volatile oxides like B₂O₃, MoO₃.

The sintering mechanism involving the formation of TiSi₂ can be explained by the following reactions:



Based on the data available for the free energy of formation of different compounds,²⁸ it was found that the overall free energy change for reaction (5) was $\Delta G_5 > 0$ at high temperature ($> 1773 \text{ K}$). Hence, the first reaction involving chemical interaction of TiO₂ and MoSi₂ resulting in the formation of TiSi₂ is not feasible thermodynamically. However, the thermodynamic calculations reveal the overall free energy change for the other possible reaction, i.e., $\Delta G_6 < 0$ at and above 1773 K (1500°C). For example, the thermodynamic calculations indicate that ΔG_6 at 1800 K is -183.018 Kcal .²⁸ At $T > 1800 \text{ K}$, ΔG_6 becomes more negative. Hence, reaction (6), leading to the formation of TiSi₂, is thermodynamically feasible. It can be noted here that this reaction can take place even at a low oxygen partial pressure, as relevant in our hot-pressing experiments. Also, XRD

results clearly indicate the formation of TiSi₂. Additionally, the weight loss measured after sintering can be correlated with the formation of volatile compounds like B₂O₃(g) and MoO₃(g), which evaporate at a hot-pressing temperature of 1700°C. The vaporization of MoO₃ is reported for oxidation of MoSi₂.²⁹

From the above discussion, it is quite likely that the densification of TiB₂ with a MoSi₂ sinter-additive occurs via liquid-phase sintering, involving the rearrangement of grains in the presence of a wetting liquid phase (TiSi₂).

(2) Mechanical Properties

A comparison of the mechanical properties of newly developed TiB₂ materials with the earlier developed materials is presented in Table II. In earlier experiments, various researchers have optimized the amount of sinter-additives like AlN, Si₃N₄ during sintering experiments and the results obtained with optimized sinter-additives, for example 2.5% Si₃N₄, 5% AlN, are also mentioned in Table II. For comparison, the material property data obtained with 10% ceramic additive are also indicated in Table II. Observing the data in Table II, it should be clear that TiB₂ materials with a combination of high hardness (25 GPa or more) and modest fracture toughness ($\sim 5 \text{ MPa} \cdot \text{m}^{1/2}$) could be achieved with the use of various non-metallic sinter-additive. When compared with TiB₂ sintered with 5% or 10% AlN sinter-additives, TiB₂-MoSi₂ exhibits higher hardness. The indentation toughness, measured with our materials, however remains modest. Importantly, one can notice that the maximum hardness achievable in TiB₂-based materials densified using a non-metallic sinter-additive is limited to around $7 \text{ MPa} \cdot \text{m}^{1/2}$ (TiB₂-5% AlN). Also, the combination of hardness and toughness obtained with the newly developed materials with a MoSi₂ sinter-additive is comparable with the earlier developed TiB₂-2.5% Si₃N₄ materials. However, when compared with TiB₂-2.5% Si₃N₄ ceramic, our materials are densified at a lower hot press temperature at 1700°C.

The indentation-induced radial crack patterns emanating from the Vickers indentations are shown in Fig. 6. In both monolith as well as TiB₂-10% MoSi₂ composites, sharp and perfect indentations are visible, and the observation of smaller Vickers indents conforms well to the measured high hardness (Fig. 6(a)). The wider residual crack opening of the Vickers indentation induced cracks in case of the TiB₂-10% MoSi₂ composite implicates a lower fracture toughness (Fig. 6(b)). Figure 6(c) provides the evidence of the deflection of indentation-induced crack by ceramic particulates. No indication of crack bridging is observed in our materials. This confirms that the crack deflection is the only toughening mechanism.

As a concluding remark, it can be said that the present study clearly indicates that MoSi₂ can be potentially used as a ceramic binder in densifying borides. While high hardness of borides can be retained in the composites, the fracture toughness remains moderate. Further research should be directed toward optimizing the silicide content in the narrow window of 0–10 wt%, while obtaining high densification and hardness. Preliminary electrical conductivity data reveal that the 20% silicide-containing boride composite has better electrical conductivity than monolithic boride. Recent thermal property measurements using the laser flash technique revealed that the TiB₂-20% MoSi₂ composite has a higher thermal conductivity of 64.8

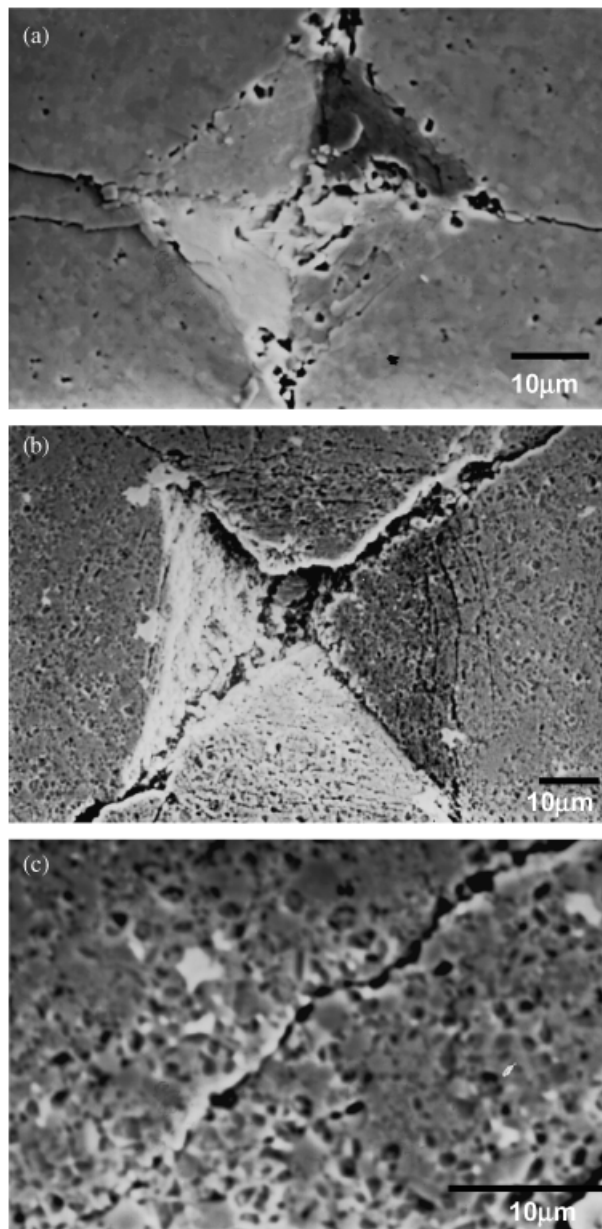


Fig. 6. SEM images showing the Vickers indentation on hot-pressed monolithic titanium boride (TiB_2) at 50 N indent load (a) and on the TiB_2 -10% MoSi_2 composite at 100 N load (b). The propagation of indentation-induced crack revealing crack deflection in the TiB_2 -10% MoSi_2 composite (c).

$\text{W} \cdot (\text{m} \cdot \text{K})^{-1}$ at 500°C .³⁰ Additionally, the unlubricated tribological testing at room temperature on a fretting tribometer indicated a higher wear resistance of the TiB_2 -20 wt% MoSi_2 composites than that of monolithic TiB_2 under varying load (2–10 N), and the dominant mechanism of material removal was identified to be tribochemical wear. The details of the friction and wear properties are reported elsewhere.³¹

From the above, it can be stated that the newly developed materials would be suitable for various engineering applications, like wear parts, high-temperature applications requiring high thermal conductivity, etc. Additionally, the high-temperature oxidation properties of TiB_2 -20% MoSi_2 composite are evaluated and compared with that of monolithic TiB_2 by our research group.³²

V. Conclusions

(a) The use of finer TiB_2 powders, synthesized by borocarbothermic reactions, and a lower hot-pressing tempera-

ture of 1800°C results in obtaining $\sim 98\%$ ρ_{th} dense binderless TiB_2 with a finer microstructure (~ 2 – $5 \mu\text{m}$), high hardness (25–26 GPa), and modest indentation fracture toughness ($5.1 \text{ MPa} \cdot \text{m}^{1/2}$).

(b) Our experimental results clearly reveal that MoSi_2 can be used as a sinter-additive for densification of TiB_2 . A high sintered density of 97% ρ_{th} is obtained in a TiB_2 -10 wt% MoSi_2 composite, hot pressed at 1700°C for 1 h. In case of pressureless sintered materials, a maximum of 91% ρ_{th} is obtained with 25% MoSi_2 composites, when sintering is carried out at 1900°C for 2 h in an inert ($\text{Ar} + \text{H}_2$) atmosphere.

(c) XRD and TEM results indicate the formation of TiSi_2 , a reaction product formed during hot pressing at 1700°C . TiSi_2 , being a liquid at hot-pressing temperature, promotes liquid-phase sintering and hence enhances densification.

(d) The optimized composite (TiB_2 -10 wt% MoSi_2) exhibits a significantly higher hardness ($H_v \sim 26.5 \text{ GPa}$) and modest indentation toughness ($K_{Ic} \sim 4.3 \text{ MPa} \cdot \text{m}^{1/2}$). The attainment of high hardness is presumably because of a finer microstructure containing TiB_2 (2–3 μm) and MoSi_2 (3–4 μm). The crack deflection is observed as the only toughening mechanism.

Acknowledgment

The authors also thank Krishanu Biswas for help with TEM investigation.

References

- R. Telle and G. Petzow, "Strengthening and Toughening of Boride and Carbide Hard Material Composites," *Mater. Sci. Eng. A*, **105/106**, 97–104 (1988).
- M. K. Ferber, P. F. Becher, and C. B. Finch, "Effect of Microstructure on the Properties of TiB_2 Ceramics," *Commun. Am. Ceram. Soc.*, **66** [1], C-2–3 (1983).
- S. Kang, D. J. Kim, E. S. Kang, and S. S. Baek, "Pressureless Sintering and Properties of Titanium Diboride Ceramics Containing Chromium and Iron," *J. Am. Ceram. Soc.*, **84** [4] 893–5 (2001).
- E. S. Kang, C. W. Jang, C. H. Lee, C. H. Kim, and D. K. Kim, "Effect of Iron and Boron Carbide on the Densification and Mechanical Properties of Titanium Diboride Ceramics," *J. Am. Ceram. Soc.*, **72** [10] 1868–72 (1989).
- L. H. Li, H. E. Kim, and E. S. Kang, "Sintering and Mechanical Properties of Titanium Diboride with Aluminum Nitride as a Sintering Aid," *J. Eur. Ceram. Soc.*, **22**, 973–7 (2002).
- R. Telle, S. Meyer, G. Petzow, and E. D. Franz, "Sintering Behavior and Phase Reactions of TiB_2 with ZrO_2 Additives," *Mater. Sci. Eng. A*, **105/106**, 125–9 (1988).
- Y. Muraoka, M. Yoshinaka, K. Hirota, and O. Yamaguchi, "Hot Isostatic Pressing of TiB_2 - ZrO_2 (2 Mol% Y_2O_3) Composite Powders," *Mater. Res. Bull.*, **31** [7] 787–92 (1996).
- S. Torizuka and T. Kishi, "Effect of SiC and ZrO_2 on Sinterability and Mechanical Properties of Titanium Nitride, Titanium Carbonitride and Titanium Diboride," *Mater. Trans. JIM.*, **37** [4] 782–7 (1996).
- T. Graziani and A. Bellosi, "Sintering and Characterization of TiB_2 - B_4C - ZrO_2 Composites," *Mater. Manufact. Processes*, **9** [4] 767–80 (1994).
- S. Torizuka, J. Harada, and H. Nishio, "High Strength TiB_2 ," *Ceram. Eng. Sci. Proc.*, **11** [9–10] 1454–60 (1990).
- J. Schneider, K.-H. Zum Gahr, R. Muller, and E.-D. Franz, "Einfluss Des ZrO_2 -Zusatzes Auf Mechanische Eigenschaften und Den Ungeschmierten Gleitverschleib von TiB_2 - ZrO_2 -Mischkeramiken," *Mater.-wiss.u.Werkstofftech.*, **27**, 359–66 (1996).
- S. Torizuka, K. Sato, J. Harada, H. Yamamoto, and H. Nishio, "Microstructure and Sintering Mechanism of TiB_2 - ZrO_2 -SiC Composite," *J. Ceram. Soc. Jpn.*, **100** [4] 392–7 (1992).
- S. Torizuka, K. Sato, H. Nishio, and T. Kishi, "Effect of SiC on Interfacial Reaction and Sintering Mechanism of TiB_2 ," *J. Am. Ceram. Soc.*, **78** [6] 1606–10 (1995).
- J. Ho Park, Y. Koh, H. Kim, C. Hwang, and E. Kong, "Densification and Mechanical Properties of Titanium Diboride with Silicon Nitride as Sintering Aid," *J. Am. Ceram. Soc.*, **82** [11] 3037–42 (1999).
- C. E. Holcombe and N. L. Dykes, "Microwave Sintering of Titanium Diboride," *J. Mater. Sci.*, **26**, 3730–8 (1991).
- E. S. Kang and C. H. Kim, "Improvements in Mechanical Properties of TiB_2 by the Dispersion of B_4C Particles," *J. Mater. Sci.*, 580–4 (1989).
- Y. Murata, H. P. Julien, and E. D. Whitney, "Densification and Wear Resistance of Ceramic Systems: I. Titanium Diboride," *Ceram. Bull.*, **46** [7] 643–8 (1967).
- S. K. Bhaumik, C. Diwakar, A. K. Singh, and G. S. Upadhyaya, "Synthesis and Sintering of TiB_2 and TiB_2 -TiC Composite Under High Pressure," *Mater. Sci. Eng. A*, **279**, 275–81 (2000).
- T. Watanabe and K. Shoubu, "Mechanical Properties of Hot-Pressed TiB_2 - ZrO_2 Composites," *J. Am. Ceram. Soc.*, **68** [2] C-34–6 (1985).
- M. Singh and H. Wiedemeier, "Chemical Interactions in Diboride-Reinforced Oxide-Matrix Composites," *J. Am. Ceram. Soc.*, **74** [4] 724–7 (1991).
- C. Subramanian and A. K. Suri, "Development of Boron Based Neutron Absorption Materials," *Met. Mater. Processes*, **16**, 39–52 (2004).

²²R. Koc and B. Hodge, "Production of TiB₂ from a Precursor Containing Carbon Coated TiO₂ and B₄C," *J. Mater. Sci. Lett.*, **19**, 667–9 (2000).

²³G. R. Anstis, P. Chantikul, B. R. Lawn, and D. B. Marshall, "A Critical Evaluation of Indentation Techniques for Measuring Fracture Toughness: I, Direct Crack Measurements," *J. Am. Ceram. Soc.*, **64** [9] 533–8 (1981).

²⁴S. Palmqvist, "Rissbildungsarbeit bei Vickers-Eindrucken als Mass fur die Zhigkeit von Hartmetallen," *Arch. Eisenhüttenwes.*, **9**, 1 (1962).

²⁵K. Biswas, B. Basu, A. K. Suri, and K. Chattopadhyay, "Tem Investigation and Densification Mechanism of Novel TiB₂-Based Composite," *J. Am. Ceram. Soc.*, 2005, Submitted.

²⁶Y.-M. Chiang, D. Birnie, and W. D. Kingery, *Physical Ceramics: Principles for Ceramic Science and Engineering*, pp. 398–404. John Wiley & Sons Inc., New York, 1997.

²⁷S. Baik and P. F. Becher, "Effect of Oxygen Contamination on Densification of TiB₂," *J. Am. Ceram. Soc.*, **70** [8] 527–30 (1987).

²⁸American Chemical Society and American Institute of Physics for the National Bureau of Standards, *JANAF Thermodynamic Tables*, 3rd edition, American Chemical Society and American Institute of Physics for the National Bureau of Standards, Midland, MI, 1985.

²⁹T. C. Chou and T. G. Nieh, "New Observations of MoSi₂ Pest at 500°C," *Scripta Metall. Mater.*, **26**, 1637–42 (1992).

³⁰T. S. R. Ch. Murthy, "Processing and Characterization of TiB₂-Based Materials"; MTech Dissertation Thesis, Indian Institute of Technology, Kanpur, India, July 2004.

³¹T. S. R. Ch. Murthy, B. Basu, Amitesh Srivastava, R. Balasubramaniam, and A. K. Suri, "Tribological Properties of TiB₂ and TiB₂-MoSi₂ Ceramic Composites," *J. Eur. Ceram. Soc.*, (2005), in press.

³²T. S. R. Ch. Murthy, R. Balasubramaniam, B. Basu, A. K. Suri, and M. N. Mungole, "Oxidation of Monolithic TiB₂ and TiB₂-20 wt% MoSi₂ Composite at 850°C," *J. Eur. Ceram. Soc.*, (2005), in press. □